Langmuir

Article

pubs.acs.org/Langmuir

Competitive Sorption Kinetics of Inhibited Endo- and Exoglucanases on a Model Cellulose Substrate

Samuel A. Maurer, Claire N. Bedbrook, and Clayton J. Radke*

Department of Chemical and Biomolecular Engineering, University of California—Berkeley, Berkeley, California 94720-1462, United States

ABSTRACT: For the first time, the competitive adsorption of inhibited cellobiohydrolase I (Cel7A, an exoglucanase) and endoglucanase I (Cel7B) from *T. longibrachiatum* is studied on cellulose. Using quartz crystal microgravimetry (QCM), sorption histories are measured for individual types of cellulases and their mixtures adsorbing to and desorbing from a model cellulose surface. We find that Cel7A has a higher adsorptive affinity for cellulose than does Cel7B. The adsorption of both cellulases becomes irreversible on time scales of 30−60 min, which are much shorter than those typically used for industrial cellulose hydrolysis. A multicomponent Langmuir kinetic model including first-order irreversible binding is proposed. Although adsorption and desorption rate constants differ between the two enzymes, the rate at which each surface enzyme irreversibly binds is identical. Because of the higher affinity of Cel7A for the cellulose surface, when Cel7A and Cel7B compete for surface sites, a significantly higher bulk concentration of Cel7B is required to achieve comparable surface enzyme concentrations. Because cellulose deconstruction benefits significantly from the cooperative activity of endoglucanases and cellobiohydrolases on the cellulose surface, accounting for competitive adsorption is crucial to developing effective cellulase mixtures.

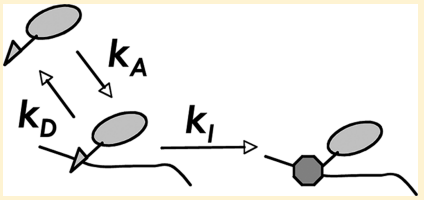

1. BACKGROUND

As humanity depletes worldwide supplies of fossil fuels, lignocellulosic biofuels offer an alternate, renewable energy source.[1−4] The rate-limiting step in lignocellulosic biofuel production is the depolymerization of biomass to form simple sugars and their oligomers that are subsequently fermented and processed to form fuel additives or other chemicals.[5−7] Currently, all industrial-scale biofuel production deploys cellulytic enzymes known as cellulases to effect depolymerization.[8] Despite a significant industrial effort toward the production of biofuels from various carbon sources, the mechanisms and kinetics that govern aqueous enzymatic deconstruction remain poorly characterized.

To develop a broader understanding of deconstruction mechanisms, we utilize a surface-based technique to measure the interfacial interaction between aqueous cellulytic enzymes and the solid cellulose surface. Most current assays of cellulase activity are performed in the bulk and therefore fail to characterize surface phenomena. Thin model films of cellulose[9] adhered to metal supports offer a well-defined surface of known area for measuring surface kinetics, whereas estimates of the enzyme-accessible surface area of the laboratory-standard cellulose Avicel can span several orders of magnitude.[10,11] Surface-based sensing techniques, such as ellipsometry,[12−15] quartz crystal microbalance,[16−21] atomic force microscopy,[22,23] Brewster angle microscopy,[24] and neutron reflectometry,[25] are then available to elucidate the mechanisms and kinetics of cellulase activity.

Cellulose is insoluble in water and recalcitrant to enzymatic degradation because of strong internal hydrogen bonding between long, nonbranching polymer chains.[26−28] Complete deconstruction of solid cellulose benefits from the concerted activity of two classes of enzymes. First, endoglucanases disrupt the hydrogen-bonding structure of cellulose and dislodge individual cellulose chain ends from the surface. Subsequently, cellobiohydrolases complex with the released chain ends, cleaving them into glucose oligomers, which are then released into aqueous solution.[29] Surface-active cellulases from these two classes each consist of a catalytic domain (CD) joined to a cellulose-binding domain (CBD) by a flexible linker. The activity of any individual cellulase can be understood according to a four-step model: (1) adsorption from bulk solution to the cellulose surface, with binding of the CBD to cellulose; (2) complexation of the active site with a cellulose chain; (3) catalytic activity within the active site; and (4) return of the cellulase to the uncomplexed adsorbed state.[12] Extended models of cellulase activity consider the cellulose chain length,[30] processive activity of cellobiohydrolases,[31] and surface diffusion of adsorbed enzymes, among other parameters.[32]

In this work, kinetic rate constants that govern the sorption of inhibited *T. longibrachiatum* cellobiohydrolase I (CBHI, Cel7A) and endoglucanase I (EGI, Cel7B) on the cellulose surface are quantified. The interaction of the CBD of these fungal cellulases with the cellulose surface, mediated by three critical tyrosine residues,[33,34] has been characterized by different sources as reversible[35] or irreversible.[36] Adsorbed proteins are well documented to evolve slowly toward irreversible attachment due to partial denaturation. To account for this slow evolution, we adopt modified Langmuir adsorption kinetics after Cascao Pereira et al.,[37] where enzymes first adsorb

Received: June 15, 2012
Revised: September 7, 2012
Published: September 11, 2012

reversibly from bulk solution to the cellulose surface, followed by slower irreversible attachment. The proposed adsorption scheme is illustrated in Figure 1.

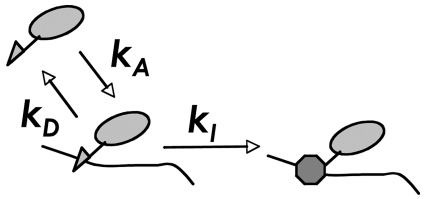

Figure 1. Schematic of cellulase sorption and irreversible binding on a cellulose surface. The cellulase catalytic domain is represented by an ellipse, and the cellulose binding domain (CBD) is shown as a triangle. Cellulase freely adsorbs and desorbs from bulk solution until it irreversibly binds, as indicated by the change in the binding domain to an octagon shape. Eventually, all adsorbed enzyme is attached irreversibly to the surface.

To measure the sorption kinetics, we implement quartz crystal microgravimetry (QCM) because it allows the characterization of small quantities of aqueous enzyme. QCM has been used previously as a continuous, noninvasive, inhibition-free, surface-oriented assay of cellulase activity. Turon et al. first utilized QCM to measure the enzymatic degradation of cellulose films.[16] Josefsson et al. studied the synergy between endoglucanases and cellobiohydrolases on the cellulose surface and generated a qualitative portrait of enzyme activity on model cellulose films.[17] Ahola et al. explored the activity of enzymes on cellulose surfaces with various deposition techniques. They fit endoglucanase adsorption kinetics to a three-parameter model.[18] Work by Hu et al. similarly explored the interaction of cellulase with several different cellulose surfaces, including the effect of concentration on the degradation rate.[19,20] Finally, Suchy et al. measured the activity of endoglucanase I on spin-coated cellulose films.[21] Despite growing interest in the use of QCM, available work is preliminary and qualitative. We provide a quantitative assessment of cellulase sorption kinetics from QCM, tracking the sorption dynamics of individual cellulases both singly and in binary mixtures.

2. MATERIALS AND METHODS

2.1. Cellulases. Isolated *T. longibrachiatum* cellulases were obtained from Megazyme (Bray, Ireland). These fungal cellulases are typical for kinetic studies of cellulytic activity.[38,39] Cellobiohydrolase I (Cel7A; Megazyme E-CBHI, MW 65 000 Da) was obtained at a concentration of 10 000 ppm in a suspension of 3.2 M ammonium sulfate/0.02 wt % ammonium azide.The *endo*-cellulase contaminant was minimal; the enzyme mixtures show 0.003 U/mg *endo*-cellulase activity in comparison to 0.1 U/mg Cel7A activity. Endoglucanase I (Cel7B; Megazyme E-CELTR, MW 57 000 Da) was obtained at a concentration of 9400 ppm in a solution of 3.2 M ammonium sulfate/0.02 wt % ammonium azide, again with minimal glucosidase contaminants. Enzymes were used as supplied after dilution to concentrations of 1−100 ppm in an aqueous solution of sodium dihydrogen phosphate buffer and glucose.

2.2. Coating and Characterization of Cellulose Films. Gold-coated QCM sensors (Q-Sense QSX-401, Västra Frölunda, Sweden) were plasma cleaned (Harrick PDC-32G; Pleasantville, NY, USA) for 10 min to remove surface organic residue. The sensors were subsequently cleaned for 5 min in a solution of distilled/deionized water, hydrogen peroxide (Sigma-Aldrich H1009, sold as a 30% w/w aqueous solution), and ammonia (Sigma-Aldrich AX1303, sold as a 30% w/w aqueous solution), mixed in a 5:1:1 volume ratio and heated to 75 °C. After rinsing with distilled/deionized water, the sensors were again plasma cleaned for 10 min to remove residual organic debris.

Thin cellulose films were deposited on the cleaned gold-coated sensors by a modification of the method of Gunnars et al.[13] Cellulose was dissolved in 4-methylmorpholine-*N*-oxide (4MMO; Sigma-Aldrich no. 224286, 97% purity) and dimethyl sulfoxide (DMSO; Sigma-Aldrich no. D5879, 99.5%) and spin-coated onto a gold sensor coated with the cationic anchor polymer poly(diallyl-dimethyl-ammonium chloride) (PDADMAC; Sigma-Aldrich no. 409030, sold as a 20% w/w aqueous solution). The cellulose film was subsequently soaked in water to remove remaining 4MMO and DMSO. The detailed procedure is available elsewhere,[12] with the following changes in solution composition: a 20 mg quantity of Avicel microcrystalline cellulose (Sigma-Aldrich no. 11363) was added to a mixture of 503 mg of powdered 4MMO and 880 mL of distilled/deionized water; after dissolution, 2 mL of DMSO was added to adjust the solution viscosity. These changes permitted the deposition of thinner, more rigid cellulose films suitable for QCM analysis. The proportion of DMSO in the coating mixture controls the viscosity of the spin-coated cellulose solution and, therefore, the mass and thickness of the adsorbed film.[12,14]

The QCM frequency response of PDADMAC-coated sensor crystals was measured before and after cellulose deposition. From the difference in the frequency response, the film mass and film thickness were ascertained. The cellulose films have an approximate dry mass of 69.5 μg and an approximate dry thickness of 42.9 ± 1.6 nm. In previous work, cellulose films prepared using this method were found to have a crystallinity of 42 ± 4%, in comparison to a crystallinity of 58 ± 2% for Avicel.[12] Our previous work also established that the cellulytic deconstruction kinetics of the model cellulose films is identical to that of their cellulose source Avicel, an industry standard for measuring enzyme activity on cellulose.[12]

2.3. Measurement of Adsorption via Quartz Crystal Microbalance. A cellulose-coated gold wafer was placed in the flow cell of a quartz crystal microbalance (QCM; Q-Sense E4, Västra Frölunda, Sweden). The flow cell was subsequently filled with a 9.5 mM NaH_2PO_4 aqueous buffer solution (pH 5.5; Sigma-Aldrich no. S9638) containing glucose (Sigma-Aldrich no. G5767) at a concentration of 6000 ppm. Glucose was added to the aqueous solution to inhibit not only cellulase activity but also cellulase complexation with cellulose, thus allowing the measurement of enzyme adsorption absent these factors.[12,40] Aqueous glucose at this concentration does not significantly affect the mass of the model cellulose films nor does it inhibit the adsorption of aqueous cellulase on the cellulose surface.[12]

The cellulose film was allowed to swell in the buffer/glucose solution until a constant frequency shift was reached, typically 1 to 2 h after exposure to the solution. Following swelling, a solution of cellulase at the desired concentration in the same buffer/glucose mixture was flowed over the cellulose-coated wafer at a flow rate of 100 μL/min, typically for 15−120 min, during which time the frequency shift and dissipation response of the cellulose film were monitored continuously. Although endoglucanase penetration into amorphous cellulose films has been reported,[25] cellulases do not penetrate the partially crystalline films used in this work, even in conjunction with cellulytic enzyme activity.[12] Thus, only external surface sorption is measured. Following the sorption step, nascent buffer/glucose solution was allowed to flow over the wafer to remove reversibly adsorbed surface enzyme. All sorption experiments were conducted at 25 °C.

2.4. QCM Frequency and Dissipation Shift. Figure 2 shows a typical frequency-shift (ΔF) and energy-dissipation (ΔD) response for a solution of 10 ppm cellobiohydrolase I (Cel7A) in glucose/buffer solution. Data for the third overtone are shown, whereas the response at the fundamental frequency was typically noisy. When the film is exposed to Cel7A, the frequency shift decreases, indicating adsorption of the enzyme to the cellulose surface. After 30 min of exposure to enzyme, buffer/glucose solution is allowed to flow across the cellulose film ($[E]_{bulk} = 0$). The frequency shift then increases, indicative of enzyme washoff. Energy dissipation, which varies with the rigidity of the film, correspondingly increases during the adsorption phase and

dx.doi.org/10.1021/la3024524 | *Langmuir* 2012, 28, 14598−14608

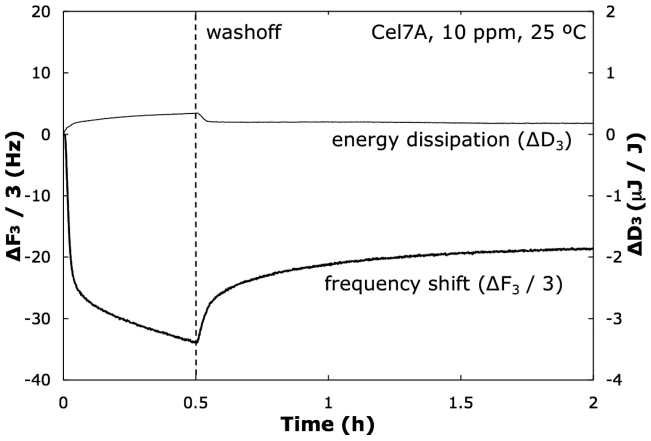

Figure 2. Typical frequency shift (ΔF, thick line) and dissipation (ΔD, thin line) histories for an enzyme loading/washoff experiment. Data were measured for the third overtone of a Q-Sense QCM operating at 5 MHz. The washoff after 30 min is indicated by a vertical dashed line. *T. longibrachiatum* Cel7A (10 ppm) with 6000-ppm glucose in aqueous buffer at 25 °C.

decreases during the washoff phase (i.e., the film becomes less rigid as cellulase adsorbs to the surface). However, the magnitude of the energy dissipation is small compared to the frequency shift.

For rigid films with a sufficiently low dissipation response, the Sauerbrey equation[41] relates the change in mass of the resonating film to the frequency-shift response

$$\Delta F = -\frac{2f_0^{\,2}}{A\sqrt{\rho_q G_q}}\Delta m \qquad (1)$$

where ΔF is the frequency shift measured by the QCM; Δm is the change in resonating mass associated with the cellulose-film surface; f_0 represents the resonance frequency of the quartz crystal (5 MHz); A denotes the area of the gold-coated sensor; ρ_q is the density of quartz (2.648 g/cm^3); and G_q represents the shear modulus of quartz (29.47 GPa).[41] Thus, the change in mass of a sufficiently rigid thin film varies linearly with the observed frequency shift. In this study, frequency-shift results were converted to adsorbed mass density (mg/m^2) using the QTools 3.01 software package included with the Q-Sense instrument. The $\Delta D/\Delta F$ ratio was 0.01−0.05 in all experiments, validating the use of the Sauerbrey equation.[41]

Increasing flow rate up to a factor of 10 had no effect on enzyme adsorption histories, verifying that mass transfer was not rate-limiting. This experimental result was further validated by using Lévêque theory to calculate the mass-transfer resistance[12] given the geometry of the QCM flow cell,[42] a flow rate of 100 μL/min (a shear rate of 0.4 s^{-1}), and an estimated enzyme diffusion coefficient of 10^{-6} cm^2/s.

Control experiments were conducted without glucose inhibition to confirm that glucose does not alter the rate of adsorption for Cel7A or Cel7B. For small adsorption times (t < 5 min), both the frequency and dissipation response were identical for cellulose films exposed to identical concentrations of both enzymes, with or without the presence of glucose inhibitor. Cellulase adsorption onto cellulose occurs more rapidly than does the complexation and degradation of surface cellulose chains.[12,31] Thus, at early exposure times with noninhibited cellulase, adsorption kinetics can be detected independently of cellulose degradation. Following the short-time exposure (t > 5 min), enzyme complexation and degradation are observed in the experiments without inhibitor. These experimental results corroborate our previous findings obtained with ellipsometry. (See Figure 6 in ref 12.) Dissolved glucose used as an inhibitor of complexation does not affect Cel7A or Cel7B adsorption on the cellulose surface. Both inhibited-enzyme adsorption and cellulytic mass-degradation rates (measured in the absence of inhibitor) agreed well when independently determined from ellipsometry[12] and here from QCM.

3. RESULTS

Figure 3 depicts typical enzyme adsorption histories for cellobiohydrolase I (Cel7A) in glucose/buffer solution at

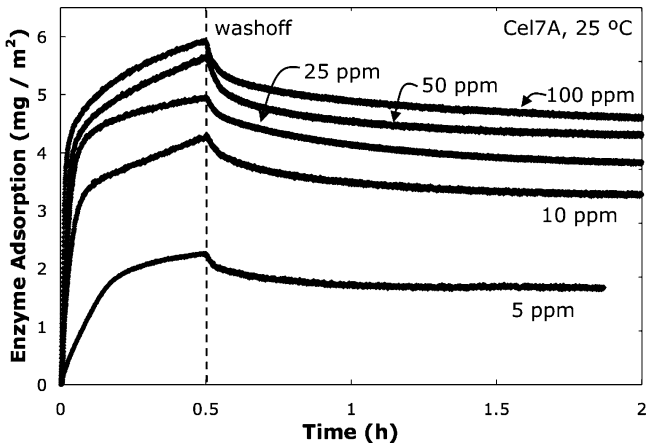

Figure 3. Loading/washoff histories for *T. longibrachiatum* Cel7A. Washoff after 30 min is indicated by a vertical dashed line. Enzyme concentrations from bottom to top are 5, 10, 25, 50, and 100 ppm. Corresponding irreversibly bound enzyme fractions after washoff are 0.72, 0.78, 0.74, 0.77, and 0.77. Cel7A with 6000-ppm glucose in aqueous buffer at 25 °C.

selected concentrations from 5 to 100 ppm. In each experiment, Cel7A adsorbed for 30 min before washoff with glucose/buffer solution. Higher concentrations of cellulase give higher surface loadings prior to washoff. Following elution, extensive flushing of the cellulose surface did not completely remove the enzyme. Rather, a sizable fraction remained irreversibly bound. For the initial 30-min exposure time, about 75% remained bound to the surface for all Cel7A concentrations studied.

Figure 4 shows similar adsorption histories for endo-β-glucanase (Cel7B) in glucose/buffer solution with washoff after 30 min and for bulk enzyme concentrations of 5−100 ppm. Again, higher Cel7B concentrations exhibit a larger 30-min

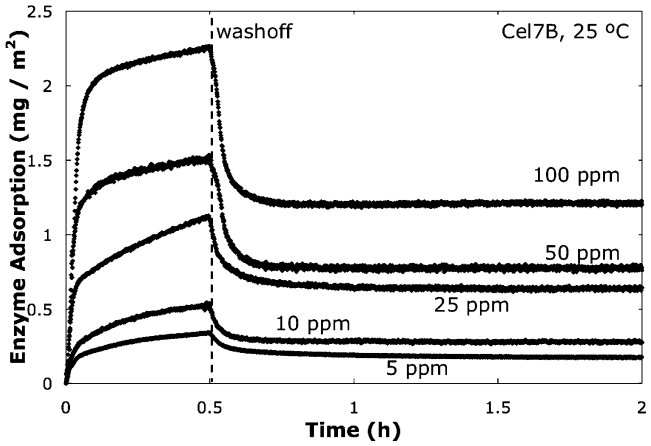

Figure 4. Loading/washoff histories for *T. longibrachiatum* Cel7B. Washoff after 30 min is indicated by a vertical dashed line. Enzyme concentrations from bottom to top are 5, 10, 25, 50, and 100 ppm. Corresponding irreversibly bound enzyme fractions after washoff are 0.55, 0.48, 0.54, 0.51, and 0.54. Cel7B with 6000-ppm in aqueous buffer at 25 °C.

dx.doi.org/10.1021/la3024524 | *Langmuir* 2012, 28, 14598−14608

surface loading, and elution only partially desorbs Cel7B. For Cel7B, about 50% remains irreversibly bound after washoff, independent of enzyme concentration. Comparison of Figures 3 and 4 indicates that the affinity of Cel7B for the cellulose surface is smaller than that of Cel7A. At 100 ppm, an adsorption of 2.4 mg/m^2 for Cel7B is reached at t = 30 min, compared to 5.9 mg/m^2 for Cel7A. Although not seen on the scales of Figures 3 and 4, the initial rates of adsorption, shown in Figure 5, are linear with bulk-solution concentration for both Cel7A and Cel7B. Figure 5 agrees with the faster adsorption kinetics for Cel7A seen in Figures 3 and 4.

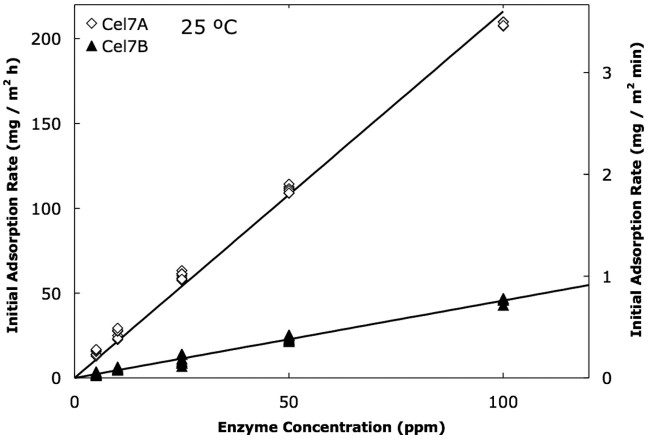

Figure 5. Initial cellulase adsorption rate (t < 3 min) on model cellulose films. *T. longibrachiatum* Cel7A (◊) and Cel7B (▲) with 6000-ppm glucose in aqueous buffer at 25 °C. Lines correspond to linear adsorption kinetics. The right axis presents the cellulase adsorption rate in minutes.

To elucidate the dynamics of irreversible adsorption, loading/elution histories of Cel7A and Cel7B were measured for differing washoff times. Figures 6 and 7 present sorption histories for single Cel7A and Cel7B enzymes at 25 ppm in glucose/buffer solution for washoff times of 3, 15, 30, and 60 min. For both enzymes, the loading kinetics follows the identical trajectory for all washoff times. The longer the enzyme is in contact with the surface before washoff, the larger is the

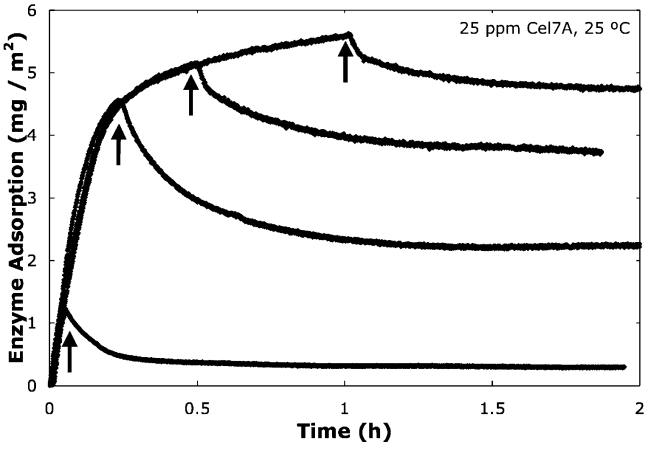

Figure 6. Loading/washoff histories for *T. longibrachiatum* Cel7A on a model cellulose film. Washoff after 3, 15, 30, and 60 min is indicated by vertical arrows. Cel7A (25 ppm) with glucose (6000 ppm) in aqueous buffer at 25 °C.

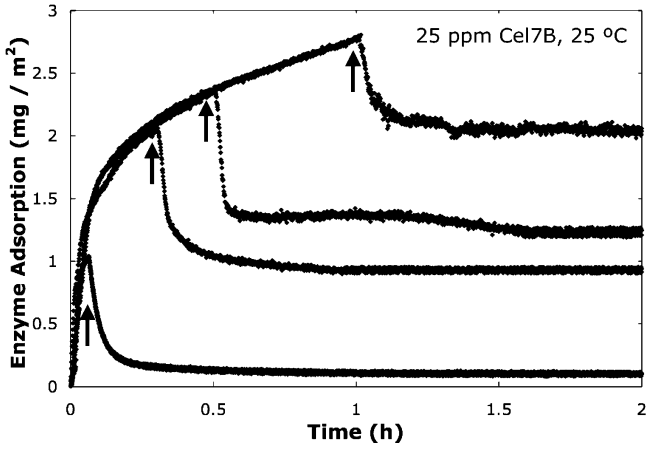

Figure 7. Loading/washoff histories for *T. longibrachiatum* Cel7B on a model cellulose film. Washoff after 3, 15, 30, and 60 min is indicated by vertical arrows. Cel7B (25 ppm) with glucose (6000 ppm) in aqueous buffer at 25 °C.

amount of enzyme that remains irreversibly bound to the surface.

Figure 8 shows the adsorption kinetics of Cel7A and Cel7B over 12 h of contact with the cellulose surface, and the inset

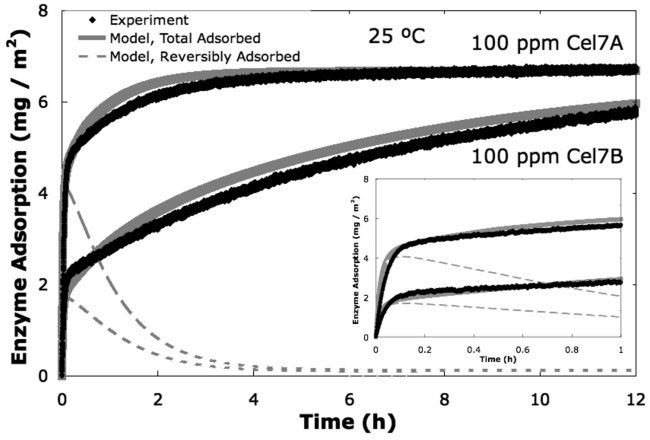

Figure 8. Adsorption histories for *T. longibrachiatum* Cel7A and Cel7B at 100 ppm with 6000 ppm glucose in aqueous buffer for times up to 12 h. The inset shows the identical data plotted over a time scale of 1 h. Smooth lines correspond to theory for total enzyme adsorption (thick gray lines) and reversible adsorption (dashed gray lines).

shows the same data plotted only up to t = 1 h. Figures 6 and 7 and the inset in Figure 8 suggest that cellulose adsorption is mainly irreversible and at a maximum level after about 2 h of exposure to the cellulose surface. The long-time adsorption kinetics shown in Figure 8, however, illustrates that the binding of the irreversibly adsorbed cellulase is prolonged and not complete even after 12 h. Smooth gray solid and dashed lines in this figure, and in those to follow, reflect the kinetic model described below. Figure 8 supports the faster adsorption of Cel7A relative to that of Cel7B at the same concentration. Noteworthy, however, is the finding that the maximum uptake of each cellulase is essentially the same, approximately 6.8 mg/m^2.

Figure 9 shows the fraction of Cel7A and Cel7B remaining irreversibly bound to the surface after washoff as a function of loading time before washoff. Lines in this figure are predicted

dx.doi.org/10.1021/la3024524 | *Langmuir* 2012, 28, 14598−14608

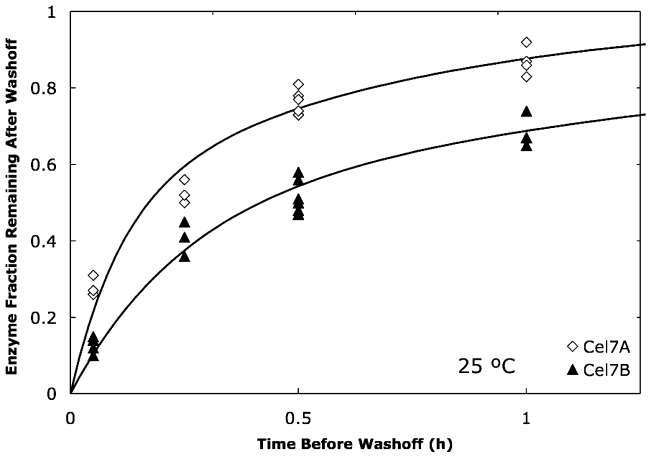

Figure 9. Fraction of cellulase irreversibly bound to a model cellulose film after washoff as a function of the time bulk cellulase solution was in contact with the surface before washoff. *T. longibrachiatum* Cel7A (◊) and Cel7B (▲) 25 ppm enzyme with 6000-ppm glucose in aqueous buffer at 25 °C. Lines correspond to theory.

from our proposed kinetic model described below. Data in Figures 8 and 9 are consistent with a framework where enzyme first binds to the surface reversibly and later inexorably transitions to an irreversibly bound state. Figure 9 also shows that the final irreversibly bound fraction for Cel7B is smaller than that for Cel7A. This is consistent with the lower affinity of Cel7B for the cellulose surface, shown in Figures 6–8. With a lower surface affinity, Cel7B desorbs more quickly than does Cel7A. Therefore, a larger proportion is washed off before it irreversibly binds.

Figure 10 plots the enzyme adsorption at 30 min of loading as a function of bulk enzyme concentration for solutions of

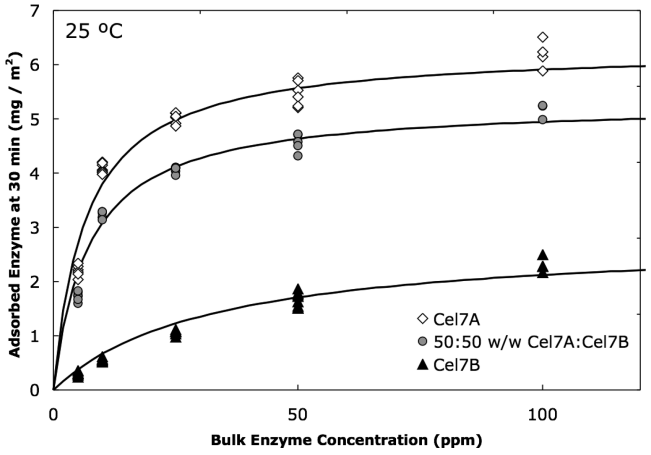

Figure 10. Adsorbed amount at 30 min for *T. longibrachiatum* single Cel7A (◊), single Cel7B (▲), and a 50:50 w/w mixture of the two enzymes (○) as a function of bulk concentration. Enzyme with 6000-ppm glucose in aqueous buffer at 25 °C. Lines correspond to kinetic theory.

Cel7A alone, Cel7B alone, and a 50:50 w/w mixture of Cel7A and Cel7B. Again, lines on this figure correspond to theory. This graph is similar in shape to a Langmuir isotherm. However, the resemblance is only apparent. The data do not truly follow a Langmuir isotherm because irreversible adsorption prevents the system from reaching an equilibrium balance between adsorption and desorption rates. In Figure 10, Cel7A exhibits an apparently higher adsorption affinity for the cellulose surface than does Cel7B, with a much larger amount adsorbed after 30 min for all bulk cellulase concentrations. Accordingly, the adsorption of the 50:50 Cel7A/Cel7B mixture is closer to that of single Cel7A than to the adsorption of single Cel7B. Figure 8, however, shows that on long time scales the final irreversibly adsorbed amount of each enzyme is the same. Thus, the results in Figure 10 arise from faster sorption kinetics for Cel7A compared to those for Cel7B. A kinetic model is necessary to quantify these observations.

4. KINETIC MODEL

4.1. Single-Enzyme Sorption Kinetics. To explain the results in Figures 3–10, we adopt a Langmuir sorption kinetic model after Cascao Pereira et al.[37] Single-enzyme data are analyzed to obtain sorption rate constants for Cel7A and Cel7B. These rate constants are then utilized to predict the sorption kinetics of the mixed enzymes.

Details of the kinetic model, illustrated in Figure 1, are available elsewhere.[37] For each single cellulase, we establish transient mass balances for the surface concentration of reversibly and irreversibly adsorbed enzyme. Using these rate expressions and the associated adsorption site balance, we establish mass balances for the surface concentration of reversibly and irreversibly adsorbed enzyme

$$\frac{d\Gamma_E}{dt} = k_A[E]_{bulk}(\Gamma_{max} - \Gamma_E - \Gamma_I) - k_D\Gamma_E - k_I\Gamma_E \quad (2)$$

$$\frac{d\Gamma_I}{dt} = k_I\Gamma_E \quad (3)$$

and

$$\Gamma_{max} = \Gamma_E + \Gamma_I + \Gamma_O \quad (4)$$

where Γ_E and Γ_I are the surface concentrations of reversibly adsorbed and irreversibly bound enzyme, respectively; $[E]_{bulk}$ is the constant bulk enzyme concentration; Γ_{max} is the maximum surface enzyme concentration; Γ_O is the surface concentration of open sites available for enzyme binding; and k_A, k_D, and k_I are rate constants for adsorption, desorption, and irreversible binding, respectively. The first two terms on the right side of eq 2 specify Langmuir adsorption and desorption rates, respectively. We assume that irreversible adsorption occurs by the transformation of the adsorbed enzyme and hence is described by first-order kinetics for irreversible sorption in eqs 2 and 3.

4.2. Single-Enzyme Kinetic Parameters. To determine k_A, the rate constant governing the adsorption of cellulase to the cellulose surface, initial rates of adsorption of cellulase to the cellulose surface are obtained immediately after the cellulose surface is exposed to enzyme (t < 2 min). Figure 5 reports measured initial enzyme adsorption amounts in the absence of prior adsorbed or irreversibly bound cellulase ($\Gamma_E \approx 0$, $\Gamma_I \approx 0$). In this case, eq 2 reduces to

$$\left.\frac{d\Gamma_E}{dt}\right|_{t\approx 0} = k_A[E]_{bulk}\Gamma_{max} \quad (5)$$

Accordingly, slopes of the lines fit to the data in Figure 5 give $k_A\Gamma_{max}$ for single Cel7A and single Cel7B initial adsorption. From Figure 8, we observe a maximum adsorption of Γ_{max} = 6.8 mg/m^2 for both Cel7A and Cel7B. It is then simple to ascertain the Cel7A and Cel7B adsorption rate constants as $k_{A,Cel7A}$ =

dx.doi.org/10.1021/la3024524 | *Langmuir* 2012, 28, 14598–14608

$0.28 \pm 0.05\ h^{-1}\ ppm^{-1}$ and $k_{A,Cel7B} = 0.070 \pm 0.013\ h^{-1}\ ppm^{-1}$, respectively.

Kinetic parameters k_D and k_I, describing the desorption and irreversible binding of cellulase on the cellulose surface, are obtained in the following manner. The total surface concentration of all states of cellulase on the cellulose surface, either reversibly adsorbed or irreversibly bound, is $\Gamma_T = \Gamma_E + \Gamma_I$. Let t_0 be the time at which washoff commences ($[E]_{bulk} = 0$), and let $\Gamma_{E,0}$, $\Gamma_{I,0}$, and $\Gamma_{T,0}$ respectively represent the corresponding surface concentrations of adsorbed cellulase, irreversibly bound cellulase, and total adsorbed cellulase. Similarly, we define $\Gamma_{E,\infty}$, $\Gamma_{I,\infty}$, and $\Gamma_{T,\infty}$ as the corresponding surface concentrations of adsorbed cellulase, irreversibly bound cellulase, and total cellulase, once washoff is complete. At infinite time, only irreversibly bound cellulase remains on the surface. Thus, by definition, $\Gamma_{T,\infty} = \Gamma_{I,\infty}$ and $\Gamma_{E,\infty} = 0$. Figure 11 defines the pertinent variables used in ascertaining k_D and k_I.

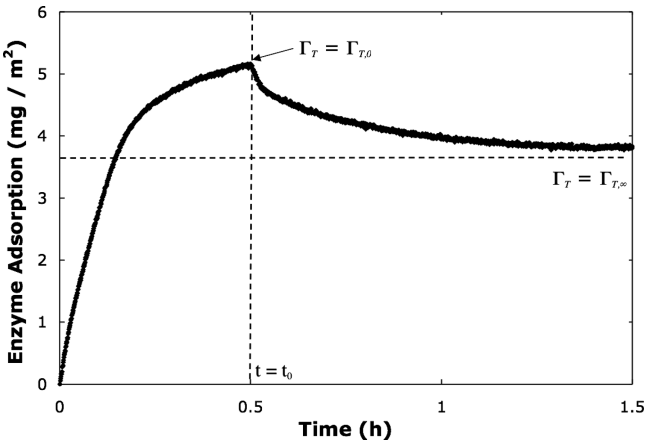

Figure 11. Definitions of t_0, $\Gamma_{T,0}$, and $\Gamma_{T,\infty}$ on a typical loading/washoff history.

Beginning with eqs 2 and 4 applied during washoff ($[E]_{bulk} = 0$), Appendix A specifies the total surface enzyme concentration as a function of time parametrized by the kinetic constants k_D and k_I:

$$\frac{\Gamma_T(t) - \Gamma_{T,\infty}}{\Gamma_{T,0} - \Gamma_{T,\infty}} = e^{-(k_D + k_I)(t - t_0)} \tag{6}$$

Importantly, eq 6 describes the total surface enzyme concentration Γ_T, not individual reversibly and irreversibly adsorbed concentrations Γ_E and Γ_I, which cannot be measured separately by QCM. Equation 6 is applied to the QCM-measured loading/elution histories to determine the washoff parameter: $k_D + k_I$. Averaged across all experiments, $k_{D,Cel7A} + k_{I,Cel7A} = 8.3 \pm 0.4\ s^{-1}$ for Cel7A and $k_{D,Cel7B} + k_{I,Cel7B} = 25.6 \pm 3.3\ s^{-1}$ for Cel7B. The value of the washoff parameter varies by less than 10% for Cel7A and 20% for Cel7B over all experiments, validating the irreversible adsorption model.

It is not possible to solve eqs 2−4 directly to obtain a closed-form expression for k_D and k_I individually. We therefore solve eqs 2−4 numerically via a Runge−Kutta algorithm to determine separate values for k_D and k_I by iterating over a limited range of values specified by experimental data. The details are discussed in Appendix B.

Resulting best-fit rate constants are listed in Table 1. We find desorption and irreversible binding rate constants of $k_{D,Cel7A} = 6.6 \pm 1.2\ s^{-1}$ and $k_{I,Cel7A} = 1.7 \pm 0.8\ s^{-1}$ for endoglucanase and $k_{D,Cel7B} = 24.0 \pm 2.8\ s^{-1}$ and $k_{I,Cel7B} = 1.6 \pm 0.5\ s^{-1}$. Example calculated loading/washoff histories for single Cel7A and single Cel7B are shown in Figure 12. All calculated histories fit the transient data well. We have also used the proposed kinetic model to predict the smooth lines shown in Figures 5 and 8−10. In all cases, excellent agreement is achieved for both transient data and data taken at single time points. In particular, note from the light-gray dashed lines in Figure 8 the rate at which the adsorbed enzymes transform to irreversible attachment. Within 1 h, well over one-half of each adsorbed enzyme is permanently attached to the surface.

Table 1. Kinetic Parameters for Single Cel7A and Cel7B

	k_A ($ppm^{-1}\ h^{-1}$)	k_D (h^{-1})	K_L (ppm^{-1})	k_I (h^{-1})
Cel7A	0.28 ± 0.05	6.6 ± 1.2	0.042 ± 0.013	1.7 ± 0.8
Cel7B	0.070 ± 0.013	24.0 ± 2.8	0.0029 ± 0.0009	1.6 ± 0.5

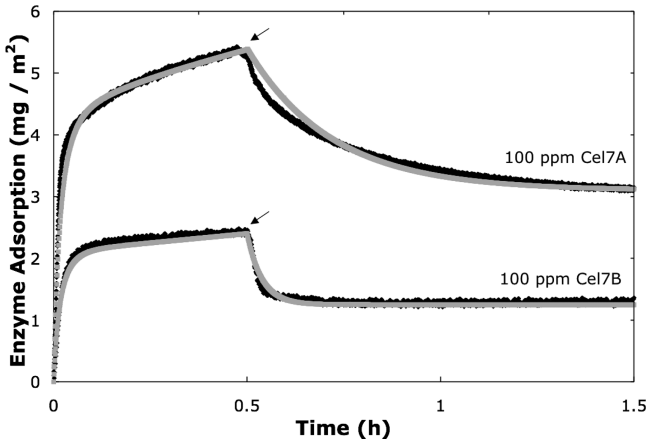

Figure 12. Example single-enzyme loading/washoff histories (black points) compared to theory (gray lines). Washoff after 30 min indicated by arrows. Cel7A and Cel7B (each 100 ppm) from *T. longibrachiatum* with 6000-ppm glucose in aqueous buffer at 25 °C. Single-enzyme kinetic constants from Table 1.

4.3. Mixed-Enzyme Sorption Kinetics. The extension of the kinetic model to the prediction of competitive loading/washoff histories is important to application. For a binary mixture of Cel7A and Cel7B, eqs 2−4 take the following forms:

$$\frac{d\Gamma_{E,Cel7A}}{dt} = k_{A,Cel7A}[Cel7A]_{bulk}\Gamma_O - k_{D,Cel7A}\Gamma_{E,Cel7A} - k_{I,Cel7A}\Gamma_{E,Cel7A} \tag{8}$$

$$\frac{d\Gamma_{I,Cel7A}}{dt} = k_{I,Cel7A}\Gamma_{E,Cel7A} \tag{9}$$

$$\frac{d\Gamma_{E,Cel7B}}{dt} = k_{A,Cel7B}[Cel7B]_{bulk}\Gamma_O - k_{D,Cel7B}\Gamma_{E,Cel7B} - k_{I,Cel7B}\Gamma_{E,Cel7B} \tag{10}$$

$$\frac{d\Gamma_{I,Cel7B}}{dt} = k_{I,Cel7B}\Gamma_{E,Cel7B} \tag{11}$$

and

$$\Gamma_{max} = \Gamma_{E,Cel7A} + \Gamma_{E,Cel7B} + \Gamma_{I,Cel7A} + \Gamma_{I,Cel7B} + \Gamma_O \tag{12}$$

dx.doi.org/10.1021/la3024524 | *Langmuir* 2012, 28, 14598−14608

Equations 8−12 are readily solved numerically for the surface concentrations of reversibly adsorbed and irreversibly bound Cel7A and Cel7B in any given mixture. As a stringent test of our mixture kinetic model, we utilize the single-enzyme rate constants to predict the kinetic behavior of binary mixtures. Figure 13 graphs modeled total cellulase adsorption, Γ_T, for

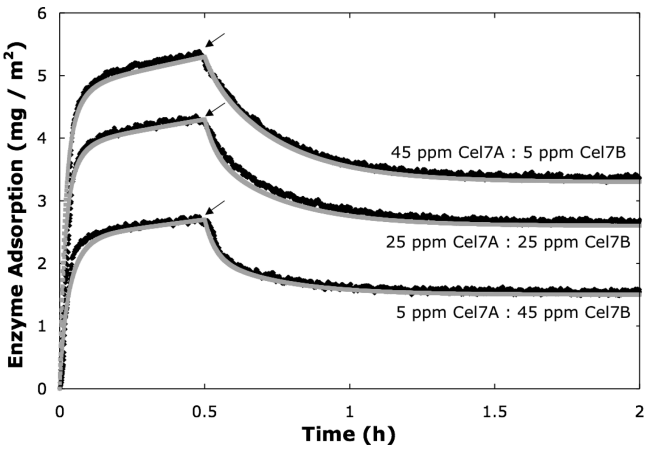

Figure 13. Loading/washoff histories (black data) for three *T. longibrachiatum* Cel7A and Cel7B mixtures on a model cellulose film compared to theory (gray lines). Washoff after 30 min is indicated by arrows. Enzyme in 6000-ppm glucose in aqueous buffer at 25 °C. Single-enzyme kinetic constants from Table 1. No adjustable parameters were used.

three such binary mixtures (45 ppm Cel7A:5 ppm Cel7B; 25 ppm Cel7A:25 ppm Cel7B; and 5 ppm Cel7A:45 ppm Cel7B) in comparison to experimental data. Excellent agreement is seen. Similar excellent agreement between the model and experiment for competitive adsorption is also seen in Figure 10. The proposed kinetic sorption model well predicts loading/washoff in a multiple-enzyme system including the competitive reduction of the lesser-adsorbing enzyme. All rate constants used in the extended two-enzyme model were obtained from single-enzyme experimental data. No additional adjustable parameters were employed in the predictions.

5. DISCUSSION

Rate constants k_A and k_D vary significantly between Cel7A and Cel7B, with k_A for Cel7A a factor of 4 higher and k_D a factor of 3.5 smaller. The Langmuir equilibrium constant $K_L = k_A/k_D$, a measure of cellulase affinity for the cellulose surface, is thus a factor of 14 larger for Cel7A. Cel7A adsorbs more readily to the cellulose surface than does Cel7B and also desorbs more slowly.

However, as shown in Figure 8, when both enzymes are left in contact with the surface for long time periods (t = 10 − 12 h), they have the same asymptotic adsorption maximum, Γ_{max} = 6.8 mg/m^2. On short time scales (t = 0−2 h), as shown in the inset of Figure 8, adsorption is limited by an apparent Langmuir equilibrium where adsorption and desorption reach an approximate balance, with irreversible adsorption playing a comparatively small role. Thus, Cel7A initially appears to reach a higher adsorption maximum than does Cel7B. However, on longer time scales (t = 10−12 h), both enzymes continue to adsorb, with slow desorption, because a large proportion of surface enzyme converts to the irreversibly bound state. At long times, adsorption is controlled primarily by steric effects, up to the observed adsorption maximum. Although Cel7A and Cel7B have different molecular weights (65 and 57 kDa), the shared mass-adsorption maximum suggests similar steric effects limit the adsorption of both cellulases. Josefsson et al. did not observe long-time adsorption but calculated an enzyme adsorption of 8.3 mg/m^2 for Cel7A and 3.7 mg/m^2 for endoglucanase V after 1 h of surface contact at similar enzyme concentrations, corroborating our observation of Cel7A having a higher surface affinity than a corresponding endoglucanase.[17] Thin films used in the work of Josefsson et al. were synthesized from dissolving pulp cellulose rather than from Avicel. Differences in surface morphology may therefore account for the observed difference in maximum Cel7A adsorption. In previous work, we utilized ellipsometry and a similar adsorption method to calculate an adsorption maximum of Γ_{max} = 2.9 mg/m^2 for a lyophilized mixture of cellulases from *T. reesei*.[12] However, this mixture of cellulases also included non-surface-active enzymes lacking cellulose-binding domains (cellobiases) and other contaminants and therefore may not have adsorbed as strongly as the isolated cellulases used in this work. The observed adsorption maximum remains below the monolayer adsorption level calculated from a typical cellulase geometry, $\Gamma_{mono} = 9.8 \times 10^{-3}$ g/m^2.[12]

Figures 3 and 4 show that for a given washoff time (t = 30 min) the proportion of enzyme remaining irreversibly bound on the cellulose surface remains constant, independent of the bulk enzyme concentration and total surface adsorption. This important finding suggests that observed irreversible binding is not caused by cellulase aggregation either in bulk solution or on the cellulose surface, which requires an increase in the irreversible binding rate at higher enzyme bulk and surface concentrations. Rather, the interactions of individual adsorbed cellulase molecules with the cellulose surface produce irreversible binding.

The first-order irreversible-binding rate constants (k_I) for Cel7A and Cel7B are approximately equal. The CBDs for Cel7A and Cel7B are structurally similar to the extent that a recombinant protein consisting of a Cel7A catalytic domain attached to a Cel7B cellulose-binding domain exhibits identical activity to that of native Cel7A.[43] Given the similar binding sites and irreversible binding rate constants, we propose that irreversible binding is governed primarily by the interaction of the CBD with the cellulose film. Adsorption of the CBD by both enzymes is mediated by the interaction of three tyrosine residues[33] with the cellulose surface, with the possible involvement of tryptophan and glutamine residues.[44] Possible mechanisms for irreversible binding include covalent interactions between aromatic CBD residues and free hydroxyl groups on the cellulose surface or morphological change/local partial surface denaturation[45,46] of the CBD. Changes in the character of tryptophan and glutamine interactions could also account for irreversible binding. Unfortunately, detailed mechanisms of adsorption for fungal cellulase CBD from solution to the cellulose surface are not well characterized. Both experimental studies[35,42,47] and molecular modeling[34,48] provide few direct, definitive descriptions of the CBD−surface interaction.

Although the irreversible binding rate constants for Cel7A and Cel7B are identical, their adsorption and desorption rate constants ($k_A$and k_D) differ. Adsorption and desorption from bulk solution, however, is not dictated solely by the CBD but also by the geometry and morphological properties of the entire cellulase molecule. Cel7A and Cel7B have different molecular weights and catalytic-domain geometries. The catalytic domain

dx.doi.org/10.1021/la3024524 | *Langmuir* 2012, 28, 14598−14608

of Cel7A is larger and resembles a binding barrel to draw in cellulose chains,[49] whereas the catalytic domain of Cel7B resembles a cleft.[50] Given the differing overall geometries, it is possible that the CBD of Cel7A contacts the surface more readily because of the orientation of the enzyme in the surface region, producing an apparent higher adsorption rate and affinity of Cel7A for the cellulose surface. The exterior of the cellulase CD may also interact with the cellulose surface,[51] providing additional binding interactions and guiding the binding of the CBD. Once adsorbed, both enzymes transition to an irreversibly bound state at the same rate, governed mostly by a change in the CBD−surface interaction.

To account for the apparent higher affinity of Cel7A for the cellulose surface despite identical binding domains and rates of irreversible adsorption, we consider the standard Gibbs free energy of enzyme adsorption to the surface,

$$\Delta G^0_{ads} = \Delta H^0_{CBD} + \Delta H^0_{CD} - T\Delta S^0_{CBD} - T\Delta S^0_{CD} \quad (13)$$

where the standard enthalpies and entropies of adsorption for cellulose binding and catalytic domains are taken as additive. Langmuir equilibrium constants in Table 1 ($K_{L,Cel7A}/K_{L,Cel7B}$ = 14) indicate a difference in the adsorption free energy of $\Delta G^0_{ads,Cel7A} - \Delta G^0_{ads,Cel7B} = -6.5$ kJ/mol. By assuming that the standard enthalpies of adsorption arise primarily from the similar CBDs and that the CDs provide only a comparatively small and not dissimilar contribution, this difference in adsorption free energy is attributed to entropic effects. The resulting standard adsorption entropy difference is then $\Delta S^0_{ads,Cel7A} - \Delta S^0_{ads,Cel7B}$ = 22 J/(mol K). Hoshino et al. find a similar adsorption entropy difference of 49 J/(mol K) for *I. lacteus* endo- and exocellulases on a cellulose surface with 60% crystallinity.[52]

It is difficult to compare our sorption rates directly to the available literature because comparable work has not employed inhibition to separate adsorption and activity kinetics. For example, Hu et al. characterized irreversible enzyme adsorption to PVAm and gold surfaces but noted that similar measurements on cellulose surfaces are difficult because desorption cannot be decoupled from cellulase activity.[19] The frequency-shift data of this group also show evidence of irreversible adsorption, although the authors suggest that it could also be attributed to a modification of the cellulose film.[19] A surface plasmon resonance (SPR) study conducted by Ma et al.[53] shows a similar quantitative picture of Cel7A adsorption as in Figure 5. Upon washoff after 5 min of contact with the surface, approximately 40% of the enzyme desorbed, with the remaining 60% left irreversibly bound to the surface. This SPR study appears to show faster enzyme adsorption and irreversible binding rates than does our study. It is possible that this results from the difference in morphology between our spin-cast cellulose films and the Whatman CF11 powdered cellulose substrate of Ma et al.[53]

6. CONCLUSIONS

Quartz crystal microgravimetry on a model cellulose film offers a continuous, noninvasive, inhibition-free assay of cellulase activity on a well-defined cellulose substrate of known surface area. Using small enzyme samples, this assay ascertains surface kinetic parameters that otherwise are impossible to obtain from traditional bulk assays on poorly defined cellulose surfaces. We quantify adsorption and desorption kinetics of single cellobiohydrolase I (Cel7A) and single endo-β-glucanase (Cel7B) under glucose inhibition on a model cellulose surface. Both Cel7A and Cel7B irreversibly bind to the cellulose surface on time scales that are as short as 3 min after exposure to the surface. Up to 90% of adsorbed enzyme is irreversibly bound after 1 h of exposure to the cellulose surface. Adsorption, desorption, and irreversible binding kinetics were characterized using an extended Langmuir sorption kinetic model. Single-enzyme rate constants successfully predict the transient loading/washoff of binary mixtures of enzymes over a range of concentration ratios with no adjustable parameters. Cel7A exhibits a higher affinity (i.e., a larger Langmuir equilibrium constant) for the surface than does Cel7B by both adsorbing more quickly and desorbing more slowly. However, the first-order rate constants governing irreversible adsorption are identical for the two enzymes. Apparently, irreversible binding is governed mainly by the interaction between the cellulose binding domain and the surface, rather than by partial denaturation of the entire two-domain enzyme. To explain the higher kinetic rates and affinity of Cel7A relative to that of Cel7B, we hypothesize that the interaction of the CBD with the cellulose surface gives similar enthalpies and entropies for each enzyme. Entropic differences of the entire molecule account for the apparently higher affinity of Cel7A for the cellulose surface. Because Cel7A and Cel7B exhibit different sorption kinetics and affinities, effective enzymatic deconstruction mixtures must be based on surface concentrations rather than on bulk concentrations. Furthermore, because both enzymes adsorb irreversibly even for relatively small exposure times, recovery and reuse of these enzymes is unlikely in a deconstruction process.

APPENDIX A: WASHOFF PARAMETER

To obtain eq 6, we write eqs 2 and 3 during washoff ($[E]_{bulk}$ = 0) and integrate eq 2 starting from $t = t_0$,

$$\Gamma_E(t) = \Gamma_{E,0} e^{-(k_D+k_I)(t-t_0)} \quad (A1)$$

This result is substituted into eq 3 and followed by integration to give

$$\Gamma_I(t) = \Gamma_{I,0} + \Gamma_{E,0}\frac{k_I}{k_D + k_I}[1 - e^{-(k_D+k_I)(t-t_0)}] \quad (A2)$$

Total adsorption, Γ_T, is the sum of Γ_E and Γ_I:

$$\Gamma_T(t) = \Gamma_{I,0} + \Gamma_{E,0}\frac{k_I}{k_D + k_I}[1 - e^{-(k_D+k_I)(t-t_0)}] + \Gamma_{E,0} e^{-(k_D+k_I)(t-t_0)} \quad (A3)$$

An evaluation of eq A3 at $t = \infty$ specifies the final total adsorption after washout,

$$\Gamma_{T,\infty} = \Gamma_{I,0} + \Gamma_{E,0}\frac{k_I}{k_D + k_I} \quad (A4)$$

and allows eq A3 to be re-expressed as eq 6 of the text.

APPENDIX B: DETERMINATION OF SINGLE RATE CONSTANTS k_D AND k_I

To set bounds on individual rate constants k_D and k_I, eq A4 is rearranged algebraically to obtain

$$\frac{\Gamma_{T,\infty} - \Gamma_{T,0}}{\Gamma_{T,0}} = \frac{\Gamma_{E,0}}{\Gamma_{T,0}}\frac{k_D}{k_D + k_I} \quad (B1)$$

dx.doi.org/10.1021/la3024524 | Langmuir 2012, 28, 14598−14608

The left side of eq B1 represents the ratio of total surface cellulase that desorbs during the washoff phase. From Figures 6 and 7, we observe that this value lies in the range of 0.1−0.8, depending on the particular cellulase studied and on the time that bulk enzyme is in contact with the surface before washoff. The first ratio on the right side of eq B1, that of reversibly adsorbed cellulase to total surface cellulase at the start of washoff, $\Gamma_{E,0}/\Gamma_{T,0}$, cannot exceed unity. Thus, the ratio $k_D/(k_D + k_I)$ must lie in the range of 0.1−1 for both Cel7A and Cel7B. Restricting the value of this ratio simplifies our parametric search for rate constants k_D and k_I.

To determine individual values for k_D and k_I, we input into the kinetic model (separately for Cel7A and Cel7B) the previously calculated values for k_A, Γ_{max}, and $k_D + k_I$. We then choose values of k_D based on the known ratio $k_D/(k_D + k_I)$. Resulting predicted loading/washoff histories were compared to those measured for various washoff times and enzyme concentrations. By iterating over the small range of possible k_D values and comparing the least-squares fit of the model to data, we obtained individual best-fit values for k_D and k_I for each cellulase, as listed in Table 1.

AUTHOR INFORMATION

Corresponding Author

*Tel: +1 510 642 5204. Fax: +1 510 642 4778. E-mail: radke@berkeley.edu.

Notes

The authors declare no competing financial interest.

ACKNOWLEDGMENTS

This work was funded by the Energy Biosciences Institute. We recognize Nick W. Brady and Neil P. Fajardo for assistance in obtaining adsorption data.

LIST OF SYMBOLS

ΔF : QCM frequency shift
ΔD : QCM energy-dissipation change
m : film mass per unit area, mg/m^2
Cel7B : *T. longibrachiatum* endoglucanase I
Cel7A : *T. longibrachiatum* cellobiohydrolase I
[E] : bulk enzyme concentration, ppm
$[Cel7B]_{bulk}$: bulk Cel7B concentration, ppm
$[Cel7A]_{bulk}$: bulk Cel7A concentration, ppm
Γ_E : surface concentration of reversibly adsorbed enzyme, mg/m^2
$\Gamma_{E,0}$: surface concentration of reversibly adsorbed enzyme at the beginning of washoff, mg/m^2
$\Gamma_{E,\infty}$: surface concentration of reversibly adsorbed enzyme at $t = \infty$, mg/m^2
Γ_{Cel7B} : surface concentration of reversibly adsorbed Cel7B, mg/m^2
Γ_{Cel7A} : surface concentration of reversibly adsorbed Cel7A, mg/m^2
Γ_I : surface concentration of irreversibly bound enzyme, mg/m^2
$\Gamma_{I,0}$: surface concentration of irreversibly bound enzyme at the beginning of washoff, mg/m^2
$\Gamma_{I,\infty}$: surface concentration of irreversibly bound enzyme at $t = \infty$, mg/m^2
$\Gamma_{Cel7A,I}$: surface concentration of irreversibly bound Cel7A, mg/m^2
$\Gamma_{Cel7B,I}$: surface concentration of irreversibly bound Cel7B, mg/m^2
Γ_{max} : maximum enzyme adsorption, mg/m^2
Γ_T : total surface concentration for all enzymes, mg/m^2
$\Gamma_{T,0}$: total surface concentration for all enzyme at the beginning of washoff, mg/m^2
$\Gamma_{T,\infty}$: total surface concentration for all enzyme at $t = \infty$, mg/m^2
Γ_O : surface concentration of open enzyme adsorption sites, mg/m^2
k_A : adsorption rate constant, ppm^{-1} h^{-1}
$k_{A,Cel7A}$: adsorption rate constant for Cel7A, ppm^{-1} h^{-1}
$k_{A,Cel7B}$: adsorption rate constant for Cel7B, ppm^{-1} h^{-1}
k_D : desorption rate constant, h^{-1}
$k_{D,Cel7A}$: desorption rate constant for Cel7A, h^{-1}
$k_{D,Cel7B}$: desorption rate constant for Cel7B, h^{-1}
k_I : irreversible binding rate constant, h^{-1}
$k_{I,Cel7A}$: irreversible binding rate constant for Cel7A, h^{-1}
$k_{I,Cel7B}$: irreversible binding rate constant for Cel7B, h^{-1}
K_L : Langmuir-type equilibrium constant, ppm^{-1}
$K_{L,Cel7A}$: Langmuir-type equilibrium constant for Cel7B, ppm^{-1}
$K_{L,Cel7B}$: Langmuir-type equilibrium constant for Cel7B, ppm^{-1}
t_0 : time point at which washoff begins

REFERENCES

(1) Himmel, M.; Ding, S. Y.; Johnson, D. K.; Adney, W. S.; Nimlos, M. R.; Brady, J. W.; Foust, T. D. Biomass Recalcitrance: Engineering Plants and Enzymes for Biofuels Production. *Science* **2007**, *315*, 804−807.

(2) Beguin, P.; Aubert, J. P. The Biological Degradation of Cellulose. *FEMS Microbiol. Rev.* **1994**, *13*, 25−58.

(3) Wyman, C. E. Ethanol from Lignocellulosic Biomass: Technology, Economics, and Opportunities. *Bioresour. Technol.* **1994**, *50*, 3−16.

(4) Houghton, J.; Weatherwax, S.; Ferrell, J. Breaking the Biological Barriers to Cellulosic Ethanol: A Joint Research Agenda. *DOE/SC-0095*: U.S. DOE: Washington, DC, 2005.

(5) Macmillan, J. D. Bioethanol Production: Status and Prospects. *Renewable Energy* **1997**, *2*−*3*, 295−302.

(6) Pauly, M.; Keegstra, K. Cell-Wall Carbohydrates and Their Modification as a Resource for Biofuels. *Plant J.* **2008**, *54*, 559−568.

(7) Kumar, R.; Singh, S.; Singh, O. V. Bioconversion of Lignocellulosic Biomass: Biochemical and Molecular Perspectives. *J Ind. Microbiol. Biotechnol.* **2008**, *35*, 377−391.

(8) Bai, F. W.; Anderson, W. A.; Moo-Young, M. Ethanol Fermentation Technologies from Sugar to Starch Feedstocks. *Biotechnol. Adv.* **2008**, *26*, 89−105.

(9) Kontturi, E.; Tammelin, T.; Österberg, M. Cellulose—Model Films and the Fundamental Approach. *Chem Soc Rev* **2006**, *35*, 1287−1313.

(10) Lee, S. B.; Shin, H. S.; Ryu, D. D. Y.; Mandels, M. Adsorption of Cellulase on Cellulose: Effect of Physicochemical Properties of Cellulose on Adsorption and Rate of Hydrolysis. *Biotechnol. Bioeng.* **1982**, *24*, 2137−2153.

(11) Abdmziem, K.; Passas, R.; Belgacem, M. N. Inverse Gas Chromatography as a Tool to Characterize the Specific Surface Area of Cellulose Fibers. *Cell Chem. Technol.* **2006**, *40*, 199−204.

(12) Maurer, S. A.; Bedbrook, C. N.; Radke, C. J. Cellulase Adsorption and Reactivity on a Cellulose Surface from Flow Ellipsometry. *Ind. Eng. Chem. Res.* **2012**, *51*, 11389−11400.

(13) Gunnars, S.; Wågberg, L.; Stuart, M. A. C. Model Films of Cellulose: I. Method Development and Initial Results. *Cellulose* **2002**, *9*, 239−249.

(14) Falt, S.; Wågberg, L.; Vesterlind, E. L.; Larsson, P. T. Model Films of Cellulose II - Improved Preparation Method and Characterization of the Cellulose Film. *Cellulose* **2004**, *11*, 151−162.
(15) Eriksson, J.; Malmsten, M.; Tiberg, F.; Callisen, T. H.; Damhus, T.; Johansen, K. S. Enzymatic Degradation of Model Cellulose Films. *J. Colloid Interface Sci.* **2005**, *284*, 99−106.
(16) Turon, X.; Rojas, O. J.; Deinhammer, R. S. Enzymatic Kinetics of Cellulose Hydrolysis: A QCM-D Study. *Langmuir* **2008**, *24*, 3880−3887.
(17) Josefsson, P.; Henriksson, G.; Wågberg, L. The Physical Action of Cellulases Revealed by a Quartz Crystal Microbalance Study Using Ultrathin Cellulose Films and Pure Cellulases. *Biomacromolecules* **2008**, *9*, 249−254.
(18) Ahola, S.; Turon, X.; Österberg, M.; Laine, J.; Rojas, O J. Enzymatic Hydrolysis of Native Cellulose Nanofibrils and Other Cellulose Model Films: Effect of Surface Structure. *Langmuir* **2008**, *24*, 11592−11599.
(19) Hu, G.; Heitmann, J. A.; Rojas, O. J. In Situ Monitoring of Cellulase Activity by Microgravimetry with a Quartz Crystal Microbalance. *J. Phys. Chem. B* **2009**, *113*, 14761−14768.
(20) Hu, G.; Heitmann, J. A.; Rojas, O. J. Quantification of Cellulase Activity Using the Quartz Crystal Microbalance Technique. *Anal. Chem.* **2009**, *81*, 1872−1880.
(21) Suchy, M.; Linder, M. B.; Tammelin, T.; Campbell, J. M.; Vuorinen, T.; Kontturi, E. Quantitative Assessment of the Enzymatic Degradation of Amorphous Cellulose by Using a Quartz Crystal Microbalance with Dissipation Monitoring. *Langmuir* **2011**, *27*, 8819−8828.
(22) Andersen, M.; Johansson, L. S.; Tanem, B. S.; Stenius, P. Properties and Characterization of Hydrophobized Microfibrillated Cellulose. *Cellulose* **2006**, *13*, 665−677.
(23) Mohan, T.; Kargl, R.; Doliska, A.; Vesel, A.; Kostler, S.; Ribitsch, V.; Stana-Kleinschek, K. Wettability and Surface Composition of Partly and Fully Regenerated Cellulose Thin Films from Trimethylsilyl Cellulose. *J. Colloid Interface Sci.* **2011**, *358*, 604−610.
(24) Habibi, Y.; Foulon, L.; Aguie-Beghin, V.; Molinari, M.; Douillard, R. Langmuir-Blodgett Films of Cellulose Nanocrystals: Preparation and Characterization. *J. Colloid Interface Sci.* **2007**, *316*, 388−397.
(25) Cheng, G.; Liu, Z.; Murton, J. K.; Jablin, M.; Dubey, M.; Majewski, K.; Halbert, C.; Browning, J.; Ankner, J.; Akgun, B.; Wang, C.; Esker, A. R.; Sale, K. L.; Simmons, B. A.; Kent, M. S. Neutron Reflectometry and QCM-D Study of the Interaction of Cellulases With Films of Amorphous Cellulose. *Biomacromolecules* **2011**, *12*, 2216−24.
(26) O'Sullivan, A. C. Cellulose: The Structure Slowly Unravels. *Cellulose* **1997**, *4*, 173−207.
(27) Gross, A.; Chu, J.-W. On the Molecular Origins of Biomass Recalcitrance: The Interaction Network and Solvation Structures of Cellulose Microfibrils. *J. Phys. Chem. B* **2010**, *114*, 13333.
(28) Cho, H. M.; Gross, A.; Chu, J.-W. Dissecting Force Interactions in Cellulose Deconstruction Reveals the Required Solvent Versatility for Overcoming Biomass Recalcitrance. *J. Am. Chem. Soc.* **2011**, *133*, 14033−14041.
(29) Zhang, Y. H. P.; Himmel, M. E.; Mielenz, J. Outlook for Cellulase Improvement: Screening and Selection Strategies. *Biotechnol. Adv.* **2005**, *24*, 452−481.
(30) Zhang, Y. H. P.; Lynd, L. R. A Functionally Based Model for Hydrolysis of Cellulose by Fungal Cellulase. *Biotechnol. Bioeng.* **2006**, *94*, 889−898.
(31) Fox, J. M.; Levine, S. E.; Blanch, H. W.; Clark, D. S. Initial- and Processive-Cut Products Reveal Cellobiohydrolase Rate Limitations and the Role of Companion Enzymes. *Biochemistry.* **2012**, *51*, 442−452.
(32) Xu, F.; Ding, H. A New Kinetic Model for Heterogeneous (Or Spatially Confined) Enzymatic Catalysis: Contributions from the Fractal and Jamming (Overcrowding) Effects. *Appl. Catal., A* **2007**, *317*, 70−81.
(33) Linder, M.; Mattinen, M. L.; Kontteli, M.; Lindeberg, G.; Stahlberg, J.; Drakenberg, T.; Reinikainen, T.; Pettersson, G.; Annila, A. Identification of Functionally Important Amino-Acids in the Cellulose-Binding Domain of *Trichoderma-reesei* Cellobiohydrolase I. *Protein Sci.* **1995**, *4*, 1056−1064.
(34) Tavagnacco, L.; Mason, P. E.; Schnupf, U.; Pitici, F.; Zhong, L. H.; Himmel, M. E.; Crowley, M.; Cesaro, A.; Brady, J. W. Sugar-Binding Sites on the Surface of the Carbohydrate-Binding Module of Cel7A from *T. reesei*. *Carbohydr. Res.* **2011**, *346*, 839−846.
(35) Linder, M.; Teeri, T. T. The Cellulose-Binding Domain of the Major Cellobiohydrolase of Trichoderma Reesei Exhibits True Reversibility and a High Exchange Rate on Crystalline Cellulose. *Proc. Natl. Acad. Sci. U.S.A.* **1996**, *93*, 12251−12255.
(36) Jung, H.; Wilson, D. B.; Walker, L. P. Binding and Reversibility of *Thermobifida fusca* Cel5A, Cel6B, and Cel48A and Their Respective Catalytic Domains to Bacterial Microcrystalline Cellulose. *Biotechnol. Bioeng.* **2003**, *84*, 151−159.
(37) Cascão Pereira, L. G.; Hickel, A.; Radke, C. J.; Blanch, H. W. A Kinetic Model for Enzyme Interfacial Activity and Stability: pa-Hydroxynitrile Lyase at the Diisopropyl Ether/Water Interface. *Biotechnol. Bioeng.* **2002**, *78*, 595−605.
(38) Levine, S. E.; Fox, J. M.; Blanch, H. W.; Clark, D. S. A Mechanistic Model of the Enzymatic Hydrolysis of Cellulose. *Biotechnol. Bioeng.* **2010**, *107*, 37−51.
(39) Bharadwaj, R.; Wong, A.; Knierim, B.; Singh, S.; Holmes, B. M.; Auer, M.; Simmons, B. A.; Adams, P. D.; Singh, A. K. High-Throughput Enzymatic Hydrolysis of Lignocellulosic Biomass via in-Situ Regeneration. *Bioresour. Technol.* **2011**, *102*, 1329−1337.
(40) Holtzapple, M.; Cognata, M.; Shu, Y.; Hendrickson, C. Inhibition of Trichoderma-Reesei Cellulase by Sugars and Solvents. *Biotechnol. Bioeng.* **1990**, *36*, 275−287.
(41) Rodahl, M.; Höök, F.; Krozer, A.; Brzezinski, P.; Kasemo, B. Quartz-Crystal Microbalance Setup for Frequency and Q-Factor Measurements in Gaseous and Liquid Environments. *Rev. Sci. Instrum.* **1995**, *66*, 3924−3930.
(42) Kwon, H. J.; Bradfield, C. K.; Dodge, B. T.; Agoki, G. S. Study of Simultaneous Fluid and Mass Adsorption Model in the QCM-D Sensor for Characterization of Biomolecular Interactions. *Proceedings of the COMSOL Conference*; Boston, 2009.
(43) Srisodsuk, M.; Lehtiö, J.; Linder, M.; Margolles-Clark, E.; Reinikainen, T.; Teeri, T. T. *Trichoderma reesei* Cellobiohydrolase I with an Endoglucanase Cellulose-Binding Domain: Action on Bacterial Microcrystalline Cellulose. *J. Biotechnol.* **1997**, *57*, 49−57.
(44) Bray, M. R.; Johnson, P. E.; Gilkes, N. R.; McIntosh, L. P.; Kilburn, D. G.; Warren, R. A. J. Probing the Role of Tryptophan Residues in a Cellulose-Binding Domain by Chemical Modification. *Protein Sci.* **1996**, *5*, 2311−2318.
(45) Soderquist, M. E.; Walton, A. G. Structural Changes in Proteins Adsorbed on Polymer Surfaces. *J. Colloid Interface Sci.* **1979**, *75*, 386−397.
(46) Castells, V.; Yang, S. X.; Van Tassel, P. R. Surface-Induced Conformational Changes in Lattice Model Proteins by Monte Carlo Simulation. *Phys. Rev. E* **2002**, *65*, 031912.
(47) Larsson, A. M.; Bergfors, T.; Dultz, E.; Irwin, D. C.; Roos, A.; Driguez, H.; Wilson, D. B.; Jones, T. A. Crystal Structure of Thermobifida busca Endoglucanase Cel6A in Complex with Substrate and Inhibitor: The Role of Tyrosine Y73 in Substrate Ring Distortion. *Biochemistry* **2005**, *44*, 12915−12922.
(48) Taylor, C. B.; Talib, M. F.; McCabe, C.; Bu, L. T.; Adney, W. S.; Himmel, M. E.; Crowley, M. F.; Becham, G. T. Computational Investigation of Glycosylation Effects on a Family 1 Carbohydrate-Binding Module. *J. Biol. Chem.* **2012**, *287*, 3147−3155.
(49) Teeri, T. T.; Reinikainen, T.; Ruohonen, L; Alwyn Jones, T.; Knowles, J. K. C. Domain Function in *Trichoderma reesei* Cellobiohydrolases. *J. Biotechnol.* **1992**, *24*, 169−176.
(50) Henrissat, B. Cellulases and Their Interaction with Cellulose. *Cellulose* **1994**, *1*, 169−196.
(51) Lin, Y.; Silvestre-Ryan, J.; Himmel, M.; Crowley, M.; Beckham, G. T.; Chu, J.-W. Protein Allostery at the Solid-Liquid Interface:

Endoglucanase Attachment to Cellulose Affects Glucan Clenching in the Binding Cleft. *J. Am. Chem. Soc.* **2011**, *133*, 16617−16624.
(52) Hoshino, E.; Kanda, T.; Sasaki, Y.; Nisizawa, K. Adsorption Mode of Exo- and Endo-Cellulases from *Irpex lacteus* (*Polyporus tulipiferae*) on Cellulose with Difference Crystallinities. *J. Biochem.* **1992**, *111*, 600−605.
(53) Ma, A.; Hu, Q.; Qu, Y.; Bai, Z.; Liu, W.; Zhuang, G. The Enzymatic Hydrolysis Rate of Cellulose Decreases with Irreversible Adsorption of Cellobiohydrolase I. *Enzyme Microb. Technol.* **2008**, *42*, 543−547.